Hybrid Beamforming Design for Multi-user mmWave Sum Rate Maximization

Chunyang Wang[1], Guannan Tan[2], Yong Fang[1], Hao Wei[3], Zhichao Sheng[1], and Hongwen Yu[1(✉)]

[1] Shanghai University, Shanghai 200444, China
{chunyangwang,yfang,zcsheng,hw_yu}@shu.edu.cn
[2] Huizhou Speed Wireless Technology Company, Huizhou 516000, China
[3] ZTE Coperation, Shenzhen 518055, China
wei.hao@zte.com.cn

Abstract. This paper considers a multi-user multiple-input-single-output (MU-MISO) mmWave downlink communication system. The hybrid beamforming (HBF) is applied at the base station (BS). A joint analog beamforming (ABF) and digital beamforming (DBF) optimization problem is formulated to maximize the sum rate (SR) of the users, the problem is generally non-convex due to the log-determinant as well as unit modulus constraints (UMC) for ABF. Two efficient alternating descent iteration algorithms are developed to solve the intractable problem. Finally, simulation results are included to verify the efficiency of the proposed approaches, results also show that the proposed algorithms can accommodate discrete phase shifts for ABF.

Keywords: Millimeter wave downlink system · Sum rate maximization · Non-convex optimization algorithm

1 Introduction

The wavelength of millimeter-wave (mmWave) is between $1-10$ mm, and its frequency band ranges from 30 GHz to 300 GHz [1]. The mmWave communication has emerged as a key technology to meet the explosive growth in data rate and quality of service (QoS) requirements in beyond fifth-generation (B5G) networks [2]. Short wavelength and a large path loss are key characteristics of mmWave communication systems. Fortunately, the small wavelength of mmWave systems allows the use of a large number of antennas, and yet achieves high array gain for directional communications by exploiting precoding techniques [3,4].

However, in the case of mmWave communication, the use of conventional fully digital beamforming is impractical. Although the optimal performance can

This work was supported by Technology Key Project of Guangdong Province, China (HZJBGS-2021001).

© ICST Institute for Computer Sciences, Social Informatics and Telecommunications Engineering 2023
Published by Springer Nature Switzerland AG 2023. All Rights Reserved
N.-S. Vo and H.-A. Tran (Eds.): INISCOM 2023, LNICST 531, pp. 104–118, 2023.
https://doi.org/10.1007/978-3-031-47359-3_8

be achieved theoretically, it is faced with the problem of high implementation complexity, large power consumption of mmWave radio frequency (RF) chains, and hardware limitations [5,6]. To address this issue, hybrid beamforming (HBF) has been proposed as an efficient approach with near-optimal performance [7–10]. The key idea of HBF is to decompose the fully digital beamforming into a high-dimensional analog beamforming (ABF) to increase the antenna gain and a low-dimensional digital beamforming (DBF) to cancel interference [11]. However, the design of HBF is extremely challenging for the reason that HBF is a product of ABF and DBF, which are coupled together. Additionally, the entries of ABF matrix are subject to the unit modulus constraint (UMC). In the studies of mmWave HBF communication systems, HBF was formulated for single-user (SU) mmWave multiple-input multiple-output (MIMO) communication [12–14]. In [12], the authors studied the beamforming design of HBF in a mmWave system. The system adopted a fully adaptive beamforming structure, wherein a switch control connection was deployed between each antenna and the RF link. In order to maximize the energy efficiency, the joint optimization problem of switching control connection and hybrid precoders was formulated as a large-scale mixed-integer non-convex problem with high dimensional power constraints. In this paper, an alternating HBF algorithm was proposed to solve continuous HBF subproblem, and then a fully adaptive HBF algorithm with matching assistance was developed to solve discrete connection-state non-convex problems. The work [13] studied a mmWave large-scale MIMO communication system and proposed a HBF scheme based on model-driven deep learning and alternating minimization. The main idea of this scheme was to maximize spectral efficiency by solving ABF and DBF alternately. In this paper, ABF network was used to solve phase shifts, and Lagrange multiplier method was used to solve DBF. The work [14] studied a mmWave MIMO communication system in order to maximize user rate. The problem was formulated and then decoupled into a series of subproblems. A method of singular value decomposition was proposed to solve the problem. However, all the aforementioned research works [12–14], only consider the simple SU communication scenario, and fail to extend the multi-user complex communication scenario.

Researchers have also remained interest in HBF design for multi-user (MU) downlink communication. The authors of [15] studied the beamforming problem in the transmission scenarios of mmWave SU MIMO communication and MU communication systems. A heuristic hybrid beamforming algorithm was proposed to maximize the sum rate (SR), and the proposed algorithm was still applicable for the case of discrete resolution. The authors in [16] studied the multi-BS and MU downlink communication system, with the aim of maximizing energy efficiency. The authors used fractional programming theory, penalty dual decomposition method, and the relationship between user rate and mean square error to transform the initial problem into a tractable problem. This optimization problem was solved by alternating direction multiplier method and block successive upper-bound minimization method. The work [17] studied mmWave MU MIMO system in a single base station (BS), and proposed a penalized dual

decomposition method to directly solve the non-convex HBF problem of the system in order to maximize spectral efficiency. The proposed algorithms can ensure convergence to Karush-Kuhn-Tucker (KKT) solution of HBF problem, which were also suitable for discrete resolution cases. However, these works [15–17] fail to provide an effective solution for UMC, which makes the calculation complexity very high.

This paper is organized as follows: In Sect. 2 and Sect. 3 respectively develop penalty optimization (PO) and alternating descent round (ADR) algorithms for the HBF design to maximize the SR. Section 4 evaluates the performance of all the algorithms. Section 5 concludes the paper.

The following inequality for all $\boldsymbol{x}$, $\bar{x}$, and positive definite $\mathbf{y}$ and $\bar{y}$ of appropriate dimension is frequently used in the paper:

$$\frac{|\boldsymbol{x}|^2}{\mathbf{y}} \geq -\frac{|\bar{x}|^4}{\bar{y}^2} + 2\frac{\bar{y}+|\bar{x}|^2}{\bar{y}^2}\Re\{\bar{x}^H\boldsymbol{x}\} - \frac{|\bar{x}|^2}{\bar{y}^2}(|\boldsymbol{x}|^2+\mathbf{y}). \tag{1}$$

2 Penalty Optimization Approach

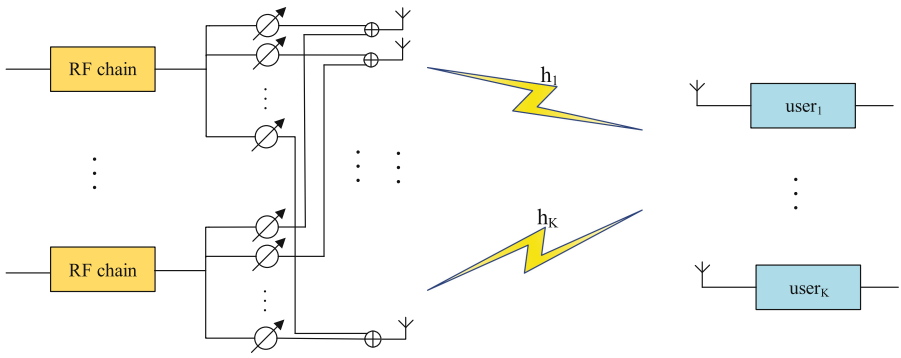

Fig. 1. MmWave MU-MISO downlink communication systems.

We consider a RIS-aided mmWave MU- MISO DL system as illustrated by Fig. 1, where the BS equips with N antennas and N_{RF} RF chains communicates with K single-antenna users, the BS is in the form of a uniform planar array (ULA) [18].

For $\mathcal{N} \triangleq \{1,\ldots,N\}$ and $\mathcal{N}_{RF} \triangleq \{1,\ldots,N_{RF}\}$, let $\boldsymbol{\theta} \triangleq [\boldsymbol{\theta}_{n,j}]_{(n,j)\in\mathcal{N}\times\mathcal{N}_{RF}} \in [0,2\pi)^{N\times N_{RF}}$ be the phase shift matrix. Define the following one-to-one mapping from $[0,2\pi)^{N\times N_{RF}}$ to $\mathbb{U}^{N\times N_{RF}} \triangleq \{\mathbf{U} = [\mathbf{u}(n,j)]_{(n,j)\in\mathcal{N}\times\mathcal{N}_{RF}} : |\mathbf{u}_{n,j}| = 1, (n,j)\in\mathcal{N}\times\mathcal{N}_{RF}\}$:

$$\begin{aligned} A(\boldsymbol{\theta}) &\triangleq \left[A^1(\boldsymbol{\theta}) \ldots A^{N_{RF}}(\boldsymbol{\theta})\right] \\ &= [e^{\jmath\boldsymbol{\theta}_{n,j}}]_{(n,j)\in\mathcal{N}\times\mathcal{N}_{RF}} \in \mathbb{U}^{N\times N_{RF}}, \end{aligned} \tag{2}$$

to represent the phase shift based ABF matrix. Due to hardware limitations, the phase shift can not take an arbitrary value, b-bit resolution is optimized, and we thus have

$$\boldsymbol{\theta}_{n,j} \in \mathcal{A} \triangleq \{0, \frac{2\pi}{2^b}, \ldots, \frac{2\pi(2^b-1)}{2^b}\}, \tag{3}$$

and the special case of $b = \infty$ corresponds to the continuous phase shifts.

For $k \in \mathcal{K} \triangleq \{1, \ldots, K\}$, $\mathbf{s} \triangleq (s_1, s_2, \ldots, s_K)$, let $s_k \in \mathbb{C}$ with $\mathbb{E}(s_k s_k^H) = I$ be the transmitted signal for user k, which is beamformed by $\mathbf{D}_k \in \mathbb{C}^{N_{RF}}$, and DBF matrix is:

$$\mathbf{D} \triangleq \left[\mathbf{D}_1 \ldots \mathbf{D}_K\right] \in \mathbb{C}^{N_{RF} \times K}, \tag{4}$$

the baseband signal x is $x = \mathbf{D}\mathbf{s} = \sum_{k=1}^{K} \mathbf{D}_k s_k$. The mmWave channel between the BS and user $k \in \mathcal{K}$ by $H_k \in \mathbb{C}^{1 \times N}$, the signal received at user k is formulated as:

$$y_k = H_k A(\boldsymbol{\theta}) \sum_{k=1}^{K} \mathbf{D}_k s_k + n_k \tag{5}$$

$$= H_k(\boldsymbol{\theta}) \sum_{k=1}^{K} \mathbf{D}_k s_k + n_k. \tag{6}$$

The HBF is given by producting of ABF $A(\boldsymbol{\theta})$ and DBF $\mathbf{D}_k$, $k \in \mathcal{K}$:

$$\mathbf{w}_k \triangleq A(\boldsymbol{\theta})\mathbf{D}_k \in \mathbb{C}^N, \tag{7}$$

and accordingly,

$$\mathbf{w} \triangleq \left[\mathbf{w}_1 \ldots \mathbf{w}_K\right] \in \mathbb{C}^{N \times K}. \tag{8}$$

According to the equations (6), the signal-to-interference-plus-noise ratio (SINR) at user k is:

$$\rho_k(\boldsymbol{\theta}, \mathbf{D}) \triangleq \frac{|H_k(\boldsymbol{\theta})\mathbf{D}_k|^2}{\sum_{l \neq k}^{K} |H_k(\boldsymbol{\theta})\mathbf{D}_l|^2 + \sigma}, \tag{9}$$

thus, the rate at user k is:

$$\mathcal{R}_k(\boldsymbol{\theta}, \mathbf{D}) \triangleq \ln(1 + \rho_k(\boldsymbol{\theta}, \mathbf{D})). \tag{10}$$

Given the power budget P, the transmit power constraint at the BS can be expressed as:

$$\sum_{k=1}^{K} ||A(\boldsymbol{\theta})\mathbf{D}_k||^2 \leq P. \tag{11}$$

The HBF design problem of maximizing the SR of users is formulated as:

$$\max_{\boldsymbol{\theta}, \mathbf{D}} \sum_{k=1}^{K} \mathcal{R}_k(\boldsymbol{\theta}, \mathbf{D}) \triangleq \max_{\boldsymbol{\theta}, \mathbf{D}} \ln\left(\prod_{k=1}^{K}(1 + \rho_k(\boldsymbol{\theta}, \mathbf{D}))\right) \tag{12a}$$

$$\text{s.t.} \quad (3), (11). \tag{12b}$$

Defining the following equation:

$$\Lambda(1+\rho_1(\boldsymbol{\theta},\mathbf{D}),\ldots,1+\rho_K(\boldsymbol{\theta},\mathbf{D})) \triangleq \prod_{k=1}^{K}(1+\rho_k(\boldsymbol{\theta},\mathbf{D})). \tag{13}$$

Let $(\theta^{(\kappa)}, D^{(\kappa)})$ be a feasible point for (13), we linearize $\Lambda(1+\rho_1(\boldsymbol{\theta},\mathbf{D}),\ldots,1+\rho_K(\boldsymbol{\theta},\mathbf{D}))$ at $(1+\rho_1(\theta^{(\kappa)},D^{(\kappa)}),\ldots,1+\rho_K(\theta^{(\kappa)},D^{(\kappa)}))$ is

$$\begin{aligned}&(1-K)\Lambda(1+\rho_1(\theta^{(\kappa)},D^{(\kappa)}),\ldots,1+\rho_K(\theta^{(\kappa)},D^{(\kappa)}))\\&+\sum_{k=1}^{K}\frac{\Lambda(1+\rho_1(\theta^{(\kappa)},D^{(\kappa)}),\ldots,1+\rho_K(\theta^{(\kappa)},D^{(\kappa)}))}{1+\rho_k(\theta^{(\kappa)},D^{(\kappa)})}(1+\rho_k(\boldsymbol{\theta},\mathbf{D})).\end{aligned} \tag{14}$$

It is plausible that this problem is equivalent to the following problem:

$$\max_{\boldsymbol{\theta},\mathbf{D}} f(\boldsymbol{\theta},\mathbf{D}) \triangleq \sum_{k=1}^{K}\gamma_k(1+\rho_k(\boldsymbol{\theta},\mathbf{D})) \tag{15a}$$

$$\text{s.t.} \qquad (3),(11), \tag{15b}$$

for

$$\gamma_k^{(\kappa)} \triangleq \frac{\Lambda(1+\rho_1(\theta^{(\kappa)},D^{(\kappa)}),\ldots,1+\rho_K(\theta^{(\kappa)},D^{(\kappa)}))}{1+\rho_k(\theta^{(\kappa)},D^{(\kappa)})}, k=1,\ldots,K, \tag{16}$$

for computational stability, $\gamma_k^{(\kappa)}$ is scaled as

$$\gamma_k^{(\kappa)} \longrightarrow \frac{\gamma_k^{(\kappa)}}{\min_{j=1,\ldots,K}\gamma_j^{(\kappa)}}, k=1,\ldots,K. \tag{17}$$

Recalling the definition (7) of HBF, the SINR of user k defined by (9) can be expressed as:

$$\rho_k(\mathbf{w}) \triangleq \frac{|H_k\mathbf{w}_k|^2}{\sum_{l\neq k}^{K}|H_k\mathbf{w}_l|^2+\sigma}, \tag{18}$$

and rate is:

$$\mathcal{R}_k(\mathbf{w}) \triangleq \ln(1+\rho_k(\mathbf{w})). \tag{19}$$

Thus, the optimization problem can be expressed as:

$$\max_{\mathbf{w}}\sum_{k=1}^{K}\mathcal{R}_k(\mathbf{w}) \triangleq \max_{\mathbf{w}}\ln(\prod_{k=1}^{K}(1+\rho_k(\mathbf{w}))) \tag{20a}$$

$$\text{s.t.} \quad \sum_{k=1}^{K}||\mathbf{w}_k||^2 \leq P, (3), (7), \tag{20b}$$

equivalence problem:

$$\max_{\mathbf{w}} f(\mathbf{w}) \triangleq \sum_{k=1}^{K} \gamma_k(1+\rho_k(\mathbf{w})) \quad \text{s.t.} \quad (3), \tag{21a}$$

$$\sum_{k=1}^{K} |\mathbf{w}_k||^2 \leq P. \tag{21b}$$

We will address (21) PO optimization problem:

$$\max_{\boldsymbol{\theta},\mathbf{D},\mathbf{w}} F(\boldsymbol{\theta},\mathbf{D},\mathbf{w}) \triangleq f(\mathbf{w}) - c||\mathbf{w}_k - A(\boldsymbol{\theta})\mathbf{D}_k||^2 \tag{22a}$$

$$\text{s.t.} \quad (3), (21b). \tag{22b}$$

with the penalty parameter c > 0 to be updated.

2.1 Hybrid Beamforming Design

We seek HBF $w^{(\kappa+1)}$ ensuring that

$$F(\theta^{(\kappa)}, D^{(\kappa)}, w^{(\kappa+1)}) > F(\theta^{(\kappa)}, D^{(\kappa)}, w^{(\kappa)}), \tag{23}$$

by considering the following problem:

$$\max_{\mathbf{w}} F(\theta^{(\kappa)}, D^{(\kappa)}, \mathbf{w}) \tag{24a}$$

$$\text{s.t.} \quad (21b). \tag{24b}$$

The following tight concave quadratic minorant is obtained by (1):

$$\begin{aligned} 1+\rho_k(\mathbf{w}) &\geq 1+\rho_k^{(\kappa)}(\mathbf{w}) \\ &\triangleq a_k^{(\kappa)} + 2b_k^{(\kappa)}\Re\{\langle c_k^{(\kappa)}\mathbf{w}_k\rangle\} - d_k^{(\kappa)}(\sum_{l=1}^{K}|H_k\mathbf{w}_l|^2), \end{aligned} \tag{25}$$

with $a_k^{(\kappa)} \triangleq -\frac{|H_k w_k^{(\kappa)}|^4}{(\sum_{l\neq k}^{K}|H_k w_l^{(\kappa)}|^2+\sigma)^2} - \sigma\frac{|H_k w_k^{(\kappa)}|^2}{(\sum_{l\neq k}^{K}|H_k w_l^{(\kappa)}|^2+\sigma)^2} + 1$, $b_k^{(\kappa)} \triangleq \frac{\sum_{l=1}^{K}|H_k w_l^{(\kappa)}|^2+\sigma}{(\sum_{l\neq k}^{K}|H_k w_l^{(\kappa)}|^2+\sigma)^2}$, $c_k^{(\kappa)} \triangleq (H_k w_k^{(\kappa)})^H H_k$, $d_k^{(\kappa)} \triangleq \frac{|H_k w_k^{(\kappa)}|^2}{(\sum_{l\neq k}^{K}|H_k w_l^{(\kappa)}|^2+\sigma)^2}$. Then we get:

$$\begin{aligned} \tilde{f}(\mathbf{w}) &\triangleq \sum_{k=1}^{K}\gamma_k^{(\kappa)}(1+\rho_k^{(\kappa)}(\mathbf{w})) - c||\mathbf{w} - A(\theta^{(\kappa)})D^{(\kappa)}||^2 \\ &\triangleq \tilde{a}^{(\kappa)} + 2\sum_{k=1}^{K}\Re\{\langle\tilde{b}_k^{(\kappa)}\mathbf{w}_k\rangle\} - \sum_{l=1}^{K}\langle Q^{(\kappa)}, [\mathbf{w}_l]^2\rangle, \end{aligned} \tag{26}$$

with $\tilde{a}^{(\kappa)} \triangleq \sum_{k=1}^{K} \gamma_k^{(\kappa)} a_k^{(\kappa)} - c||A(\theta^{(\kappa)})D^{(\kappa)}||^2$, $\tilde{b}_k^{(\kappa)} \triangleq \gamma_k^{(\kappa)} b_k^{(\kappa)} c_k^{(\kappa)} + c(D_k^{(\kappa)})^H A^H(\theta^{(\kappa)})$, $Q^{(\kappa)} \triangleq \sum_{k=1}^{K} \gamma_k^{(\kappa)} d_k^{(\kappa)} H_k^H H_k + cI_N$. We get following optimization problem:

$$\max_{\mathbf{w}} \tilde{f}(\mathbf{w}) \tag{27a}$$

$$\text{s.t.} \quad (21b), \tag{27b}$$

we use Lagrangian gradient method:

$$w_k^{(\kappa+1)} = \begin{cases} (Q^{(\kappa)})^{-1}(\tilde{b}_k^{(\kappa)})^H & \text{if} \quad \sum_{k=1}^{K} ||(Q^{(\kappa)})^{-1}(\tilde{b}_k^{(\kappa)})^H||^2 \le P \\ \left(Q^{(\kappa)} + \mu I_N\right)^{-1} (\tilde{b}_k^{(\kappa)})^H & \text{otherwise,} \end{cases} \tag{28}$$

where $\mu > 0$ is chosen such that

$$\sum_{k=1}^{K} || \left(Q^{(\kappa)} + \mu I_N\right)^{-1} (\tilde{b}_k^{(\kappa)})^H||^2 = P. \tag{29}$$

According to [19], we have closed-form solution.

2.2 Analog Beamforming Design

We seek HBF $w^{(\kappa+1)}$ ensuring that

$$F(\theta^{(\kappa+1)}, D^{(\kappa)}, w^{(\kappa+1)}) > F(\theta^{(\kappa)}, D^{(\kappa)}, w^{(\kappa+1)}), \tag{30}$$

which is equivalent to

$$-||w^{(\kappa+1)} - A(\theta^{(\kappa+1)})D^{(\kappa)}||^2 > -||w^{(\kappa+1)} - A(\theta^{(\kappa)})D^{(\kappa)}||^2, \tag{31}$$

by considering the following problem:

$$\max_{\boldsymbol{\theta}} \varphi^{(\kappa)}(\boldsymbol{\theta}) \triangleq -||w_k^{(\kappa+1)} - A(\boldsymbol{\theta})D_k^{(\kappa)}||^2 \tag{32}$$

$$\text{s.t.} \quad (3). \tag{33}$$

We have

$$\begin{aligned} \varphi^{(\kappa)}(\boldsymbol{\theta}) &= -||w^{(\kappa+1)}||^2 + 2\Re\{\langle D^{(\kappa)}(w^{(\kappa+1)})^H A(\boldsymbol{\theta})\rangle\} \\ &\quad -\langle [D^{(\kappa)}]^2 A^H(\boldsymbol{\theta}) A(\boldsymbol{\theta})\rangle \\ &= -||w^{(\kappa+1)}||^2 + 2\Re\{\langle D^{(\kappa)}(w^{(\kappa+1)})^H A(\boldsymbol{\theta})\rangle\} \\ &\quad -\lambda^{(\kappa)} N N_{RF} + \left[\lambda^{(\kappa)} ||A(\boldsymbol{\theta})||^2 - \langle [D^{(\kappa)}]^2 A^H(\boldsymbol{\theta}) A(\boldsymbol{\theta})\rangle\right] \\ &\ge -||w^{(\kappa+1)}||^2 - \lambda^{(\kappa)} N N_{RF} + 2\Re\{\langle D^{(\kappa)}(w^{(\kappa+1)})^H A(\boldsymbol{\theta})\rangle\} \\ &\quad + \Big[2\Re\{\lambda^{(\kappa)}\langle A^H(\theta^{(\kappa)}) A(\boldsymbol{\theta})\rangle\} - 2\Re\{\langle [D^{(\kappa)}]^2 A^H(\theta^{(\kappa)}) A(\boldsymbol{\theta})\rangle\} \\ &\quad -\lambda^{(\kappa)} N N_{RF} + \langle [D^{(\kappa)}]^2 A^H(\theta^{(\kappa)}) A(\theta^{(\kappa)})\rangle\Big] \qquad (34) \\ &= \hat{a}^{(\kappa)} + 2\Re\{\langle A^{(\kappa)} A(\boldsymbol{\theta})\rangle\}, \qquad (35) \end{aligned}$$

with $\lambda^{(\kappa)} \triangleq \lambda_{\max}([D^{(\kappa)}]^2)$, $\hat{a}^{(\kappa)} \triangleq -||w^{(\kappa+1)}||^2 - 2\lambda^{(\kappa)}NN_{RF} + \langle[D^{(\kappa)}]^2 A^H(\theta^{(\kappa)})A(\theta^{(\kappa)})\rangle$, $A^{(\kappa)} \triangleq D^{(\kappa)}(w^{(\kappa+1)})^H + \lambda^{(\kappa)}A^H(\theta^{(\kappa)}) - [D^{(\kappa)}]^2 A^H(\theta^{(\kappa)})$, then we get:

$$\max_{\boldsymbol{\theta}} \varphi^{(\kappa)}(\boldsymbol{\theta}) \tag{36a}$$

$$\text{s.t.} \quad (3), \tag{36b}$$

and

$$\theta^{(\kappa+1)} = \left[2\pi - \lfloor \angle A^{(\kappa)}(j,n) \rceil_b\right]_{(n,j)\in\mathcal{N}\times\mathcal{N}_{RF}}. \tag{37}$$

According to [19], we have closed-form solution.

2.3 Digital Beamforming Design

DBF can be found by

$$\begin{aligned} D^{(\kappa+1)} &= \arg\max_{\mathbf{D}} F(\theta^{(\kappa+1)}, \mathbf{D}, w^{(\kappa+1)}) \\ &= \arg\min_{\mathbf{D}} ||w^{(\kappa+1)} - A(\theta^{(\kappa+1)})\mathbf{D}||^2 \\ &= (A^H(\theta^{(\kappa+1)})A(\theta^{(\kappa+1)}))^{-1}A^H(\theta^{(\kappa+1)})w^{(\kappa+1)}. \end{aligned} \tag{38}$$

Algorithm 1. PO Algorithm

1: **Initialization:** Initialize $\theta^{(0)}$, $D^{(0)}$, and $w^{(0)}$. Set $\kappa = 0$ and $c = c_0$.
2: **Repeat until** $||w^{(\kappa)} - A(\theta^{(\kappa)})D^{(\kappa)}||^2 \leq K10^{-3}$**:** Generate $w^{(\kappa+1)}$ by (28). Generate $\theta^{(\kappa+1)}$ by (37) , and $D^{(\kappa+1)}$ by (38). If $||w^{(\kappa+1)} - A(\theta^{(\kappa+1)})D^{(\kappa+1)}||^2 > 0.9||w^{(\kappa)} - A(\theta^{(\kappa)})D^{(\kappa)}||^2$, reset $c := 1.2c$. Reset $\kappa := \kappa + 1$.
3: **Output** $w^{(\kappa)}$, $\theta^{(\kappa)}$ and $D^{(\kappa)}$. Reset

$$D^{(\kappa)} \to t_0 D^{(\kappa)}, t_0 = \sqrt{P/||A(\theta^{(\kappa)})D^{(\kappa)}||^2}.$$

3 Alternating Descent Round Approach

Based on (9) defined by:

$$\rho_k(\boldsymbol{\theta}, \mathbf{D}) \triangleq \frac{|H_k A(\boldsymbol{\theta})\mathbf{D}_k|^2}{\sum_{l\neq k}^{K} |H_k A(\boldsymbol{\theta})\mathbf{D}_l|^2 + \sigma}, \tag{39}$$

the rate at user k is:

$$\mathcal{R}_k(\boldsymbol{\theta}, \mathbf{D}) \triangleq \ln(1 + \rho_k(\boldsymbol{\theta}, \mathbf{D})). \tag{40}$$

Thus, the optimization problem can be expressed as:

$$\max_{\boldsymbol{\theta},\mathbf{D}} \sum_{k=1}^{K} \mathcal{R}_k(\boldsymbol{\theta},\mathbf{D}) \triangleq \max_{\boldsymbol{\theta},\mathbf{D}} \ln(\prod_{k=1}^{K}(1+\rho_k(\boldsymbol{\theta},\mathbf{D}))) \text{s.t.} \quad (3),(11), \tag{41a}$$

$$|\theta_{m,n}|^2 \leq 1, n=1,\ldots,N; m=1,\ldots,N_{RF}, \tag{41b}$$

accordingly, the rquivalence problem:

$$\max_{\boldsymbol{\theta},\mathbf{D}} \tilde{f}(\boldsymbol{\theta},\mathbf{D}) \triangleq \sum_{k=1}^{K} \gamma_k^{(\kappa)}(1+\rho_k(\boldsymbol{\theta},\mathbf{D})) \tag{42a}$$

$$\text{s.t.} \quad (3),(11),(41b). \tag{42b}$$

According to [20], we have the following penalized optimization problem:

$$\max_{\boldsymbol{\theta},\mathbf{D}} \hat{f}(\boldsymbol{\theta},\mathbf{D}) \triangleq \tilde{f}(\boldsymbol{\theta},\mathbf{D}) + \mu(\frac{1}{NN_{RF}} - \frac{1}{\sum_{m=1}^{N}\sum_{n=1}^{N_{RF}}|\theta_{m,n}|^2}) \tag{43a}$$

$$\text{s.t.} \quad (3),(11),(41b). \tag{43b}$$

3.1 Digital Beamforming Design

We seek $D^{(\kappa+1)}$ such that

$$\tilde{f}(\theta^{(\kappa)}, D^{(\kappa+1)}) > \tilde{f}(\theta^{(\kappa)}, D^{(\kappa)}), \tag{44}$$

using the inequality (1), then we get:

$$\begin{aligned} 1+\rho_k(\theta^{(\kappa)},\mathbf{D}) &\geq 1+\rho_k^{(\kappa)}(\mathbf{D}) \\ &\triangleq a_k^{(\kappa)} + 2b_k^{(\kappa)}\Re\{\langle c_k^{(\kappa)}\mathbf{D}_k\rangle\} - d_k^{(\kappa)}(\sum_{l=1}^{K}|H_kA(\theta^{(\kappa)})\mathbf{D}_l|^2), \end{aligned} \tag{45}$$

with $a_k^{(\kappa)} \triangleq -\frac{|H_kA(\theta^{(\kappa)})D_k^{(\kappa)}|^4}{(\sum_{l\neq k}^{K}|H_kA(\theta^{(\kappa)})D_l^{(\kappa)}|^2+\sigma)^2} - \sigma\frac{|H_kA(\theta^{(\kappa)})D_k^{(\kappa)}|^2}{(\sum_{l\neq k}^{K}|H_kA(\theta^{(\kappa)})D_l^{(\kappa)}|^2+\sigma)^2} + 1$, $b_k^{(\kappa)} \triangleq \frac{\sum_{l=1}^{K}|H_kA(\theta^{(\kappa)})D_l^{(\kappa)}|^2+\sigma}{(\sum_{l\neq k}^{K}|H_kA(\theta^{(\kappa)})D_l^{(\kappa)}|^2+\sigma)^2}$, $c_k^{(\kappa)} \triangleq (H_kA(\theta^{(\kappa)})D_k^{(\kappa)})^H H_kA(\theta^{(\kappa)})$, $d_k^{(\kappa)} \triangleq \frac{|H_kA(\theta^{(\kappa)})D_k^{(\kappa)}|^2}{(\sum_{l\neq k}^{K}|H_kA(\theta^{(\kappa)})D_l^{(\kappa)}|^2+\sigma)^2}$. Then we get:

$$\begin{aligned} \hat{f}(\mathbf{D}) &\triangleq \sum_{k=1}^{K}\gamma_k^{(\kappa)}(1+\rho_k^{(\kappa)}(\mathbf{D})) \\ &\triangleq \sum_{k=1}^{K}\gamma_k^{(\kappa)}a_k^{(\kappa)} + 2\sum_{k=1}^{K}\gamma_k^{(\kappa)}b_k^{(\kappa)}\Re\{\langle c_k^{(\kappa)}\mathbf{D}_k\rangle\} - \sum_{l=1}^{K}\langle Q^{(\kappa)},[\mathbf{D}_l]^2\rangle, \end{aligned} \tag{46}$$

with $Q^{(\kappa)} \triangleq \sum_{k=1}^{K}\gamma_k^{(\kappa)}A^H(\theta^{(\kappa)})H_k^HH_kA(\theta^{(\kappa)})$, We solve th following convex problem at κ-th iteration to generate $D_k^{(\kappa+1)}$:

$$\max_{\mathbf{D}} \hat{f}(\mathbf{D}) \tag{47a}$$

$$\text{s.t.} \quad (11). \tag{47b}$$

3.2 Analog Beamforming Design

Similarly, we seek $\theta^{(\kappa+1)}$ such that

$$\tilde{f}(\theta^{(\kappa+1)}, D^{(\kappa+1)}) > \tilde{f}(\theta^{(\kappa+1)}, D^{(\kappa+1)}), \tag{48}$$

using the inequality (1), then we get:

$$\begin{aligned} 1+\rho_k(\boldsymbol{\theta}, D^{(\kappa+1)}) &\geq 1+\tilde{\rho}_k^{(\kappa)}(\boldsymbol{\theta}) \\ &\triangleq \tilde{a}_k^{(\kappa)} + 2\tilde{b}_k^{(\kappa)}\Re\{\langle \tilde{c}_k^{(\kappa)} A(\boldsymbol{\theta})\rangle\} - \tilde{d}_k^{(\kappa)}(\sum_{l=1}^{K}|H_k A(\boldsymbol{\theta}) D_l^{(\kappa+1)}|^2 \end{aligned} \tag{49}$$

with $\tilde{a}_k^{(\kappa)} \triangleq -\frac{|H_k(\theta^{(\kappa)})D_k^{(\kappa+1)}|^4}{(\sum_{l\neq k}^{K}|H_k(\theta^{(\kappa)})D_l^{(\kappa+1)}|^2+\sigma)^2} - \sigma\frac{|H_k(\theta^{(\kappa)})D_k^{(\kappa+1)}|^2}{(\sum_{l\neq k}^{K}|H_k(\theta^{(\kappa)})D_l^{(\kappa+1)}|^2+\sigma)^2} + 1$, $\tilde{b}_k^{(\kappa)} \triangleq \frac{\sum_{l=1}^{K}|H_k(\theta^{(\kappa)})D_l^{(\kappa+1)}|^2+\sigma}{(\sum_{l\neq k}^{K}|H_k(\theta^{(\kappa)})D_l^{(\kappa+1)}|^2+\sigma)^2}$, $\tilde{c}_k^{(\kappa)} \triangleq D_k^{(\kappa+1)}(H_k(\theta^{(\kappa)})D_k^{(\kappa+1)})^H H_k$, $\tilde{d}_k^{(\kappa)} \triangleq \frac{|H_k(\theta^{(\kappa)})D_k^{(\kappa+1)}|^2}{(\sum_{l\neq k}^{K}|H_k(\theta^{(\kappa)})D_l^{(\kappa+1)}|^2+\sigma)^2}$. We thus have

$$\begin{aligned} \hat{f}(\boldsymbol{\theta}) &\triangleq \sum_{k=1}^{K}\gamma_k(1+\tilde{\rho}_k^{(\kappa)}(\boldsymbol{\theta})) \\ &= \tilde{a} + 2\Re\{\tilde{A}^{(\kappa)}A(\boldsymbol{\theta})\} - \langle \tilde{B}^{(\kappa)}, A(\boldsymbol{\theta})\tilde{C}^{(\kappa)}A^H(\boldsymbol{\theta})\rangle, \end{aligned} \tag{50}$$

with $\tilde{a}^{(\kappa)} \triangleq \sum_{k=1}^{K}\gamma_k^{(\kappa)}\tilde{a}_k^{(\kappa)}$, $\tilde{A}^{(\kappa)} \triangleq \sum_{k=1}^{K}\gamma_k^{(\kappa)}\tilde{b}_k^{(\kappa)}\tilde{c}_k^{(\kappa)}$, $\tilde{B}^{(\kappa)} \triangleq \sum_{k=1}^{K}\gamma_k^{(\kappa)}\tilde{d}_k^{(\kappa)}H_k^H H_k$, $\tilde{C}^{(\kappa)} \triangleq \sum_{l=1}^{K}[D_l^{(\kappa+1)}]^2$.

and

$$\frac{1}{\sum_{m=1}^{N}\sum_{n=1}^{N_{RF}}|\theta_{m,n}|^2} \leq \phi(\boldsymbol{\theta}) \triangleq \frac{1}{\sum_{m=1}^{N}\sum_{n=1}^{N_{RF}}(2\Re\{(\theta_{m,n}^{(\kappa)})^*\theta_{m,n}\} - |\theta_{m,n}^{(\kappa)}|^2)} \tag{51}$$

over the trust region

$$\sum_{m=1}^{N}\sum_{n=1}^{N_{RF}}(2\Re\{(\theta_{m,n}^{(\kappa)})^*\theta_{m,n}\} - |\theta_{m,n}^{(\kappa)}|^2) > 0, \tag{52}$$

we solve the following optimization problem at the κ-th iteration to generate $\theta^{(\kappa+1)}$:

$$\max_{\boldsymbol{\theta}} g^{(\kappa)}(\boldsymbol{\theta}) \triangleq [\hat{f}(\boldsymbol{\theta}) + \mu(\frac{1}{NN_{RF}} - \phi(\boldsymbol{\theta}))] \tag{53a}$$

$$\text{s.t.} \quad (3), (41b), \sum_{m=1}^{N}\sum_{n=1}^{N_{RF}}(2\Re\{(\theta_{m,n}^{(\kappa)})^*\theta_{m,n}\} - |\theta_{m,n}^{(\kappa)}|^2) > 0, \tag{53b}$$

and determine μ by

$$\mu = \frac{\gamma^{(0)}}{\frac{1}{\sum_{m=1}^{N}\sum_{n=1}^{N_{RF}}|\theta_{m,n}^{(0)}|^2} - \frac{1}{NN_{RF}}}, \tag{54}$$

to make the values of the objective function and penalty term in (43) of similar magnitudes [21].

Algorithm 2. ADR Algorithm

1: **Initialization:** Initialize $(\theta^{(0)}, D^{(0)})$.
2: **Repeat until convergence of the objective function in (42):** Generate $\theta^{(\kappa+1)}$, $D^{(\kappa+1)}$, and μ by (47), (53) and (54). Reset $\kappa := \kappa + 1$.
3: **Output** $(\theta^{(opt)}, D^{(opt)}) = (\theta^{(\kappa)}, D^{(\kappa)})$.

4 Numerical Results

With the users randomly located within the cell radius of 200 meters. The path-loss of user k experienced at a distance d_k from the BS is set to $\rho_k = 36.72 + 35.3 \log 10(d_k)$dB taking into account a 16.5 dB gain due to multiple-antenna mmWave transmission [22,23]. The mmWave channel $H_k \in \mathbb{C}^{1\times N}$ between the BS and UE k in (5) is modelled by [18]

$$H_k = \sqrt{10^{-\rho_k/10}} \sqrt{\frac{N}{N_c N_{sc}}} \sum_{c=1}^{N_c} \sum_{\ell=1}^{N_{sc}} \alpha_{k,c,\ell} a_r\left(\phi^r_{k,c,\ell}\right) a_t^H\left(\phi^t_{k,c,\ell}\right), \tag{55}$$

where N_c is the number of scattering clusters, N_{sc} is the number of scatterers within each cluster, and $\alpha_{k,c,\ell} \sim \mathcal{CN}(0,1)$ is the complex gain of the ℓth path in the cth cluster between the BS and user k. Under the classic uniform linear array antenna configuration having half-wavelength antenna spacing, the steering vectors $a_t\left(\phi^t_{k,c,\ell}\right)$ and $a_r\left(\phi^r_{k,c,\ell}\right)$ are defined by

$$a_t\left(\phi^t_{k,c,\ell}\right) = \frac{1}{\sqrt{N}}\left[1, e^{j\pi \sin\phi^t_{k,c,\ell}}, \ldots, e^{j\pi(N-1)\sin\phi^t_{k,c,\ell}}\right]^T, \tag{56}$$

and

$$a_r\left(\phi^r_{k,c,\ell}\right) = \frac{1}{\sqrt{N_R}}\left[1, e^{j\pi \sin\phi^r_{k,c,\ell}}, \ldots, e^{j\pi(N_R-1)\sin\phi^r_{k,c,\ell}}\right]^T, \tag{57}$$

where $\phi^t_{k,c,\ell}$ ($\phi^r_{k,c,\ell}$, resp.) is the azimuth angle of departure (arrival, resp.) for the ℓth path in the cth cluster from the BS to UE k, which is generated according to the Laplacian distribution in conjunction with random mean cluster angles in the interval $[0, 2\pi)$ and spreads of 10 degrees within each cluster. As in [23], we set $N_c = 5$ and $N_{sc} = 10$. The carrier frequency is set to 28 GHz, the noise power density is set to -174 dBm/Hz, while the bandwidth is set to B = 100 MHz. Unless otherwise stated, $b = 3$, $P = 15$ dBm, $N_{RF} = 8$, $K = 8$ and $N = 64$ are used. The results are multiplied by $\log_2 e$ to convert the unit nats/sec into the unit bps/Hz. The convergence tolerance of the proposed algorithms is set to 10^{-3}.

- PO: This result simulates the performance of algorithm 1 with continuous phase at the θ.
- 3-bit PO: This result simulates the performance of algorithm 1 with 3-bit discrete phase at the θ.

– ADR: This result simulates the performance of algorithm 2 with continuous phase at the θ.
– 3-bit ADR: This result simulates the performance of algorithm 2 with 3-bit discrete phase at the θ.

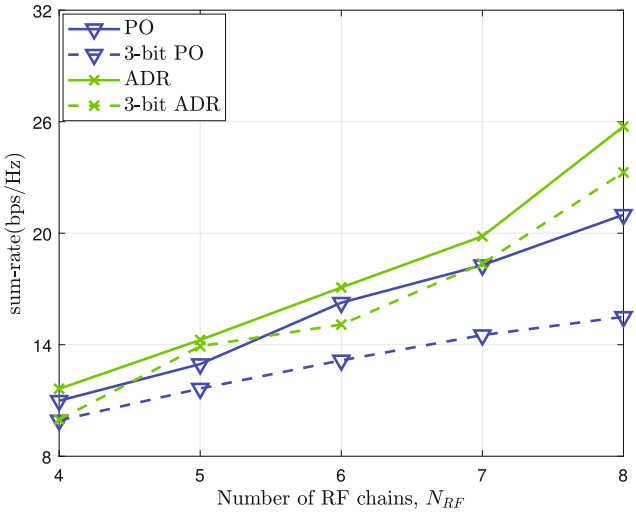

Fig. 2. SR vs the number of RF chains.

Figure 2 plots the SR under different number of RF chains for the proposed algorithms. From the point of view of the continuous phase shifts, ADR has the best SR, which outperforms PO all the time. From the point of view of the discrete phase shifts, their 3-bit resolution algorithms follow the same trend.

Figure 3, which plots the SR under different numbers of BS antennas N. PO better than ADR for $N = 16$, while ADR has the best performance for $N \geq 32$, and among 3-bit resolution algorithms 3-bit ADR has the best performance.

We also examine the SR under different BS transmit power P in Fig. 4. As expected, all the algorithms benefit from increasing the number of transmit power. And they have the same trend follow Fig. 2.

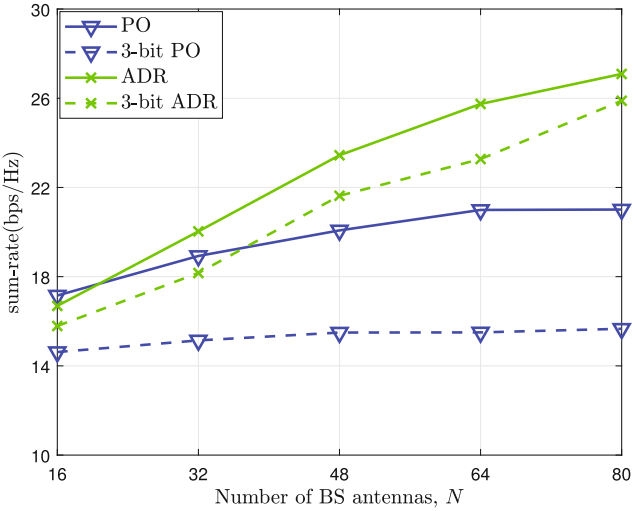

Fig. 3. SR vs the number of BS antennas.

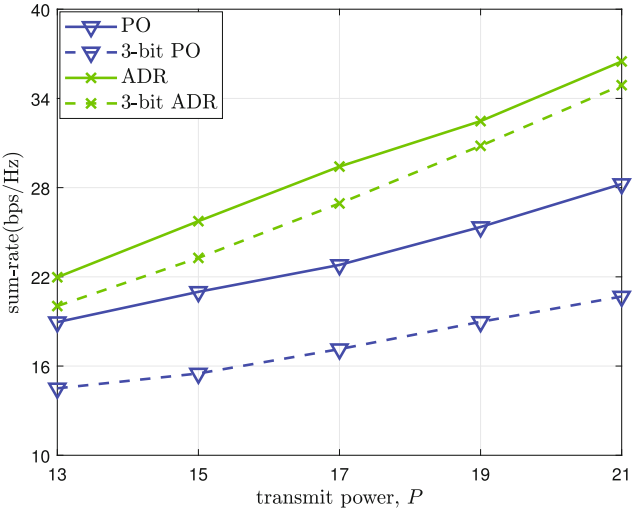

Fig. 4. SR vs the BS transmit power.

5 Conclusions

In this paper, we considered a mmWave MU-MISO downlink communication network, the objective is to maximize the SR by jointly optimizing ABF and DBF. The formulated non-convex optimization problem was solved by using the proposed alternating descent iteration algorithms. Simulation results were provided to demonstrate the superiority of our proposed algorithm.

References

1. Zhang, W., Xia, X., Fu, Y., Bao, X.: Hybrid and full-digital beamforming in mmWave massive MIMO systems: a comparison considering low-resolution ADCS. China Commun. **16**(6), 91–102 (2019)
2. Abdallah, A., Celik, A., Mansour, M.M., Eltawil, A.M.: Deep learning based frequency-selective channel estimation for hybrid mmWave MIMO systems. IEEE Trans. Wirel. Commun. **21**, 3804–3821 (2021)
3. Nguyen, N.T., Lee, K.: Coverage and cell-edge sum-rate analysis of mmWave massive MIMO systems with ORP schemes and MMSE receivers. IEEE Trans. Signal Process. **66**(20), 5349–5363 (2018)
4. Guo, R., Cai, Y., Zhao, M., Shi, Q., Champagne, B., Hanzo, L.: Joint design of beam selection and precoding matrices for mmWave mu-MIMO systems relying on lens antenna arrays. IEEE J. Select. Topics Signal Process. **12**(2), 313–325 (2018)
5. Pang, L., et al.: Joint power allocation and hybrid beamforming for downlink mmWave-NOMA systems. IEEE Trans. Veh. Tech. **70**(10), 10173–10184 (2021)
6. Li, H., Li, M., Liu, Q., Swindlehurst, A.L.: Dynamic hybrid beamforming with low-resolution PSS for wideband mmWave MIMO-OFDM systems. IEEE J. Select. Areas Commun. **38**(9), 2168–2181 (2020)
7. Heath, R.W., Gonzalez-Prelcic, N., Rangan, S., Roh, W., Sayeed, A.M.: An overview of signal processing techniques for millimeter wave MIMO systems. IEEE J. Select. Topics Signal Process. **10**(3), 436–453 (2016)
8. Busari, S.A., Huq, K.M.S., Mumtaz, S., Dai, L., Rodriguez, J.: Millimeter-wave massive MIMO communication for future wireless systems: a survey. IEEE Commun. Surv. Tut. **20**(2), 836–869 (2017)
9. Roh, W., et al.: Millimeter-wave beamforming as an enabling technology for 5g cellular communications: theoretical feasibility and prototype results. IEEE Commun. Mag. **52**(2), 106–113 (2014)
10. Li, M., Wang, Z., Li, H., Liu, Q., Zhou, L.: A hardware-efficient hybrid beamforming solution for mmWave MIMO systems. IEEE Wirel. Commun. **26**(1), 137–143 (2019)
11. Gao, X., Dai, L., Han, S., Chih-Lin, I., Heath, R.W.: Energy-efficient hybrid analog and digital precoding for mmWave MIMO systems with large antenna arrays. IEEE J. Sel. Areas Commun. **34**(4), 998–1009 (2016)
12. Xue, X., Wang, Y., Yang, L., Shi, J., Li, Z.: Energy-efficient hybrid precoding for massive mmWave MIMO systems with a fully-adaptive-connected structure. IEEE Trans. Commun. **68**(6), 3521–3535 (2020)
13. Luo, J., Fan, J., Zhang, J.: MDL-ALTMIN: A hybrid precoding scheme for mmWave systems with deep learning and alternate optimization. IEEE Wirel. Commun. Lett. **11**(9), 1925–1929 (2022)
14. Ni, W., Dong, X., Lu, W.-S.: Near-optimal hybrid processing for massive MIMO systems via matrix decomposition. IEEE Trans. Signal Process. **65**(15), 3922–3933 (2017)
15. Sohrabi, F., Yu, W.: Hybrid digital and analog beamforming design for large-scale antenna arrays. IEEE J. Select. Topics Signal Process. **10**(3), 501–513 (2016)
16. He, S., Wang, J., Huang, W., Huang, Y., Xiao, M., Zhang, Y.: Energy-efficient transceiver design for cache-enabled millimeter-wave systems. IEEE Trans. Commun. **68**(6), 3876–3889 (2020)
17. Shi, Q., Hong, M.: Spectral efficiency optimization for millimeter wave multiuser MIMO systems. IEEE J. Select. Topics Signal Process. **12**(3), 455–468 (2018)

18. El Ayach, O., Rajagopal, S., Abu-Surra, S., Pi, Z., Heath, R.W.: Spatially sparse precoding in millimeter wave MIMO systems. IEEE Trans. Wirel. Commun. **13**(3), 1499–1513 (2014)
19. Tuy, H.: Convex Analysis and Global Optimization, 2nd edn. Springer International, Cham (2017). https://doi.org/10.1007/978-3-319-31484-6
20. Yu, H., Tuan, H.D., Nasir, A.A., Duong, T.Q., Poor, H.V.: Joint design of reconfigurable intelligent surfaces and transmit beamforming under proper and improper gaussian signaling. IEEE J. Sel. Areas Commun. **38**(11), 2589–2603 (2020)
21. Shi, Y., Tuan, H.D., Tuy, H., Su, S.: Global optimization for optimal power flow over transmission networks. J. Glob. Optim. **69**(3), 745–760 (2017)
22. Rappaport, T.S., Xing, Y., MacCartney, G.R., Molisch, A.F., Mellios, E., Zhang, J.: Overview of millimeter wave communications for fifth-generation (5G) wireless networks with a focus on propagation models. IEEE Trans. Antenn. Propag. **65**(12), 6213–6230 (2017)
23. Akdeniz, M.R., et al.: Millimeter wave channel modeling and cellular capacity evaluation. IEEE J. Select. Areas Commun. **32**(6), 1164–1179 (2014)